ISSN 1948-0210 (online)

World Journal of *Stem Cells*

World J Stem Cells 2020 March 26; 12(3): 168-240

Published by Baishideng Publishing Group Inc

World Journal of Stem Cells

Contents

Monthly Volume 12 Number 3 March 26, 2020

World Journal of Stem Cells
Volume 12 Number 3 March 26, 2020

Contents

NAME OF JOURNAL
World Journal of Stem Cells

ISSN
ISSN 1948-0210 (online)

LAUNCH DATE
December 31, 2009

FREQUENCY
Monthly

EDITORS-IN-CHIEF
Tong Cao, Shengwen Calvin Li, Carlo Ventura

EDITORIAL BOARD MEMBERS
https://www.wjgnet.com/1948-0210/editorialboard.htm

EDITORIAL OFFICE
Jin-Lei Wang, Director

PUBLICATION DATE
March 26, 2020

INSTRUCTIONS TO AUTHORS
https://www.wjgnet.com/bpg/gerinfo/204

GUIDELINES FOR ETHICS DOCUMENTS
https://www.wjgnet.com/bpg/GerInfo/287

GUIDELINES FOR NON-NATIVE SPEAKERS OF ENGLISH
https://www.wjgnet.com/bpg/gerinfo/240

PUBLICATION MISCONDUCT
https://www.wjgnet.com/bpg/gerinfo/208

ARTICLE PROCESSING CHARGE
https://www.wjgnet.com/bpg/gerinfo/242

STEPS FOR SUBMITTING MANUSCRIPTS
https://www.wjgnet.com/bpg/GerInfo/239

ONLINE SUBMISSION
https://www.f6publishing.com

World Journal of Stem Cells

Submit a Manuscript: https://www.f6publishing.com

World J Stem Cells 2020 March 26; 12(3): 203-221

DOI: 10.4252/wjsc.v12.i3.203

ISSN 1948-0210 (online)

ORIGINAL ARTICLE

Basic Study

Efficient differentiation of vascular smooth muscle cells from Wharton's Jelly mesenchymal stromal cells using human platelet lysate: A potential cell source for small blood vessel engineering

Panagiotis Mallis, Aggeliki Papapanagiotou, Michalis Katsimpoulas, Alkiviadis Kostakis, Gerasimos Siasos, Eva Kassi, Catherine Stavropoulos-Giokas, Efstathios Michalopoulos

ORCID number: Panagiotis Mallis (0000-0001-9429-190X); Aggeliki Papapanagiotiou (0000-0001-6156-2128); Michalis Katsimpoulas (0000-0001-8083-3878); Alkiviadis Kostakis (0000-0003-1263-6607); Gerasimos Siasos (0000-0001-7601-8870); Eva Kassi (0000-0001-7491-2297); Catherine Stavropoulos-Giokas (0000-0003-0698-6061); Efstathios Michalopoulos (0000-0002-1901-6294).

Author contributions: Mallis P designed and carried out the whole experimental procedure of this study; Papanagiotou A, Siassos G and Kassi E supervised the differentiation procedures of MSCs into VSMCs; Katsimpoulas M and Kostakis A supervised the decellularization procedures of human umbilical arteries; Michalopoulos E designed, supervised and corrected the whole manuscript; Stavropoulos-Giokas C supervised and approved the whole study.

Institutional review board statement: This study was reviewed and approved by the Bioethics Committee of Biomedical Research Foundation Academy of Athens (Reference No. 1440, 20/11/2018).

Conflict-of-interest statement: The authors declare no conflict of interest.

Data sharing statement: Informed consent regarding the experiments

Panagiotis Mallis, Catherine Stavropoulos-Giokas, Efstathios Michalopoulos, Hellenic Cord Blood Bank, Biomedical Research Foundation Academy of Athens, Athens 11527, Greece

Aggeliki Papapanagiotou, Gerasimos Siasos, Eva Kassi, Department of Biological Chemistry, Medical School, National and Kapodistrian Univesity of Athens, Athens 15772, Greece

Michalis Katsimpoulas, Alkiviadis Kostakis, Center of Experimental Surgery, Biomedical Research Foundation Academy of Athens, Athens 11527, Greece

Gerasimos Siasos, First Department of Cardiology, "Hippokration" Hospital, University of Athens Medical School, Athens 15231, Greece

Eva Kassi, First Department of Internal Medicine, Laiko Hospital, Medical School, National and Kapodistrian University of Athens, Athens 11527, Greece

Corresponding author: Panagiotis Mallis, MSc, PhD, Hellenic Cord Blood Bank, Biomedical Research Foundation Academy of Athens, 4 Soranou Ephessiou Street, Athens 11527, Greece. pmallis@bioacademy.gr

Abstract

BACKGROUND

The development of fully functional small diameter vascular grafts requires both a properly defined vessel conduit and tissue-specific cellular populations. Mesenchymal stromal cells (MSCs) derived from the Wharton's Jelly (WJ) tissue can be used as a source for obtaining vascular smooth muscle cells (VSMCs), while the human umbilical arteries (hUAs) can serve as a scaffold for blood vessel engineering.

AIM

To develop VSMCs from WJ-MSCs utilizing umbilical cord blood platelet lysate.

METHODS

WJ-MSCs were isolated and expanded until passage (P) 4. WJ-MSCs were properly defined according to the criteria of the International Society for Cell and Gene Therapy. Then, these cells were differentiated into VSMCs with the use of platelet lysate from umbilical cord blood in combination with ascorbic acid, followed by evaluation at the gene and protein levels. Specifically, gene expression profile analysis of VSMCs for *ACTA2*, *MYH11*, *TGLN*, *MYOCD*, *SOX9*,

of the current study was received from all mother participants.

Manuscript source: Invited manuscript

Received: November 1, 2019
Peer-review started: November 1, 2019
First decision: December 12, 2019
Revised: January 17, 2020
Accepted: January 31, 2020
Article in press: January 31, 2020
Published online: March 26, 2020

P-Reviewer: Kim BS, Wang MY
S-Editor: Dou Y
L-Editor: Filipodia
E-Editor: Xing YX

NANOG homeobox, *OCT4* and *GAPDH*, was performed. In addition, immunofluorescence against ACTA2 and MYH11 in combination with DAPI staining was also performed in VSMCs. HUAs were decellularized and served as scaffolds for possible repopulation by VSMCs. Histological and biochemical analyses were performed in repopulated hUAs.

RESULTS
WJ-MSCs exhibited fibroblastic morphology, successfully differentiating into "osteocytes", "adipocytes" and "chondrocytes", and were characterized by positive expression (> 90%) of CD90, CD73 and CD105. In addition, WJ-MSCs were successfully differentiated into VSMCs with the proposed differentiation protocol. VSMCs successfully expressed *ACTA2, MYH11, MYOCD, TGLN* and *SOX9*. Immunofluorescence results indicated the expression of ACTA2 and MYH11 in VSMCs. In order to determine the functionality of VSMCs, hUAs were isolated and decellularized. Based on histological analysis, decellularized hUAs were free of any cellular or nuclear materials, while their extracellular matrix retained intact. Then, repopulation of decellularized hUAs with VSMCs was performed for 3 wk. Decellularized hUAs were repopulated efficiently by the VSMCs. Biochemical analysis revealed the increase of total hydroyproline and sGAG contents in repopulated hUAs with VSMCs. Specifically, total hydroxyproline and sGAG content after the 1st, 2nd and 3rd wk was 71 ± 10, 74 ± 9 and 86 ± 8 μg hydroxyproline/mg of dry tissue weight and 2 ± 1, 3 ± 1 and 3 ± 1 μg sGAG/mg of dry tissue weight, respectively. Statistically significant differences were observed between all study groups ($P < 0.05$).

CONCLUSION
VSMCs were successfully obtained from WJ-MSCs with the proposed differentiation protocol. Furthermore, hUAs were efficiently repopulated by VSMCs. Differentiated VSMCs from WJ-MSCs could provide an alternative source of cells for vascular tissue engineering.

Key words: Vascular smooth muscle cells; Decellularized umbilical arteries; Mesenchymal stromal cells; *MYOCD*; Cardiovascular disease; Blood vessels

Core tip: In this study, mesenchymal stromal cells derived from the Wharton's Jelly tissue were differentiated into vascular smooth muscle cells (VSMCs). For this purpose, unlike the current literature, cord blood platelet lysate was used as the key element for the differentiation of mesenchymal stromal cells into VSMCs. Furthermore, the functional evaluation of VSMCs was tested. To do this, human umbilical arteries were decellularized and repopulated with the generated VSMCs.

Citation: Mallis P, Papapanagiotou A, Katsimpoulas M, Kostakis A, Siasos G, Kassi E, Stavropoulos-Giokas C, Michalopoulos E. Efficient differentiation of vascular smooth muscle cells from Wharton's Jelly mesenchymal stromal cells using human platelet lysate: A potential cell source for small blood vessel engineering. *World J Stem Cells* 2020; 12(3): 203-221
URL: https://www.wjgnet.com/1948-0210/full/v12/i3/203.htm
DOI: https://dx.doi.org/10.4252/wjsc.v12.i3.203

INTRODUCTION

Small diameter vascular grafts with inner diameter less than 6 mm are currently applied in various surgical operations, globally[1,2]. Among them, cardiovascular disease (CAD) is estimated to affect more than 18 million people[2]. Indeed, more than 500000 bypass surgeries are performed each year, worldwide[3,4]. Primary therapeutic treatment is the replacement of damaged or obstructed coronary arteries with autologous or synthetic vascular grafts. Both approaches are characterized by several limitations[3,4]. Autologous grafts, such as saphenous vein, are only available in less

than 40% of patients with CAD, and are characterized by significantly altered biocompatibility properties[3,4].

On the other hand, synthetic vascular grafts, derived from expanded polytetrafluorethylene and Dacron, are well applied for large diameter vascular applications, although small diameter graft replacement still requires further clarification[5]. Most of the time, new surgical operations are required for these patients. When more than one vascular conduit is needed, the above therapeutic strategies cannot be applied[6,7]. Moreover, small diameter vascular grafts are required for solid organ transplantation, such as kidney and liver, in order to achieve proper revascularization and nutrient supplementation[7].

Due to the broad use of small diameter blood vessels, alternative sources must be established, thus overcoming the above limitations. Vascular graft engineering, which has attracted great interest from scientific societies, could contribute to this direction[8-10]. Decellularization of vessels and their repopulation with specific cellular populations could produce properly defined tissue engineered grafts[10-12]. For this purpose, human umbilical arteries (hUAs) with inner diameters of 1-4 mm could ideally be decellularized and possibly serve as a vascular scaffold for possible seeding by cellular populations[3,4]. HUAs are contained in human umbilical cord (hUC), a tissue that is discarded after gestation[3,4]. Normally, hUC contains two arteries and one vein that playsignificant roles in fetal blood circulation[13,14]. HUAs are vessels without any branches throughout their entire length, and can be non-invasively isolated from hUCs[15].

To date, several groups have successfully decellularized hUAs, and characterized them as small diameter vascular grafts[3,16-19]. However, the repopulation of these conduits requires further evaluation. Of particular note, these decellularized vascular grafts must be repopulated with vascular cell populations, such as endothelial cells (ECs) and vascular smooth muscle cells (VSMCs), in order to be fully functional[20,21].

In this context, VSMCs are responsible for vasoconstriction and vasodilation, and can switch from a contractile to synthetic phenotype[22]. Contractile VSMCs maintain their functional properties, such as regulation of blood pressure and blood redistribution, in response to biochemical stimuli, and are mostly found in healthy blood vessels[23]. On the other hand, synthetic VSMCs exhibit enhanced proliferation, migration, and osteochondrogenic conversion[22,23]. Synthetic VSMCs are related to vascular pathologies such as inflammation, atherosclerosis and CAD[23]. Between these two states, different genes are expressed in VSMCs. Specifically, under normal conditions, contractile phenotypes of VSMCs is regulated by the expression of *MYOCD*, *ACTA2*, *MYH11* and *TGLN*. On the other hand, under pathological conditions, a switch from a contractile to synthetic phenotype occurs, followed by *SOX9* upregulation[23]. It is known that *SOX9* expression can lead to extracellular matrix (ECM) protein synthesis[23]. Due to their significant role in vessel homeostasis, a strategy to obtain VSMCs that can be used in small diameter vascular graft engineering must be established. Unfortunately, autologous VSMCs are difficult to obtain at desired numbers from mature vessels, and their *in vitro* expansion potential is limited[23]. A large number of research groups has tried to produce VSMCs derived either from mesenchymal stromal cells (MSCs) or from induced pluripotent stem cells (iPSCs) using defined factors[24-28]. Traditional methods rely on the exogenous supplementation of biochemical induction factors[23]. However, these approaches are expensive and could cause endotoxin contamination, while iPSC technology has not been approved by the Food and Drug Administration for broad human use[23]. Taking into consideration the above data, and in order to develop functional small diameter vascular grafts, we introduced an alternative protocol for producing VSMCs from MSCs derived from Wharton's Jelly tissue (WJ-MSCs), which relied on the use of human platelet lysate (PL) from umbilical cord blood (UCB). Previous work in our laboratory conducted in UCB-PL showed significant amounts of several growth factors such as TGF-β1, PDGFA, FGF2, IFN-γ and TNF-α[29]. These growth factors have previously been used extensively in the differentiation process of MSCs to VSMCs by several groups[24-28]. In addition, UCB-PL is free of any animal-derived substances such as prions, peptides and proteins, which can cause zoonotic infections or allergic reactions. In this way, the produced VSMCs might be better tolerated by patients. Also, UCB-PL has exhibited beneficial properties as s supplement for MSC isolation and expansion[29]. The aim of this study was to produce VSMCs from WJ-MSCs using the UCB-PL, in order to serve as a potential source of cells for vascular tissue engineering. Initially WJ-MSCs were isolated, characterized according to the International Society for Cell and Gene Therapy (ISCT) standards[30], and differentiated into VSMCs. In parallel, hUAs were isolated from hUCs, decellularized, and then histologically and biochemically evaluated. Differentiated VSMCs were initially evaluated at the gene and protein levels, and then used for the repopulation of decellularized hUAs. The efficacy of repopulation was defined with both

histological and biochemical assays.

MATERIALS AND METHODS

Isolation of hUAs and WJ tissue

The hUCs (n = 10) used in this study for the isolation of hUAs and WJ tissues were derived from normal and caesarian deliveries with gestational ages 38-40 wk. Each hUC was accompanied by informed consent. The informed consent was signed by the mothers a few days before delivery, was in accordance with the Helsinki declaration, and conformed with the ethical standards of the Greek National Ethical Committee. The overall study has been approved by our Institution's ethical board (Reference No. 1440. November 20th, 2018). The hUCs were delivered to the Hellenic Cord Blood Bank in less than 48 h, and proceeded immediately to the isolation of hUAs and WJ tissues. Briefly, the hUCs were rinsed in phosphate buffer saline 1× (PBS 1×, Sigma-Aldrich, Darmstadt, Germany) for removal of excessive blood and blood clots. Sterile instruments were used for the isolation of hUAs and WJ tissues. Then, hUAs and WJ tissue were kept separately in 15 mL polypropylene falcon tubes (BD Biosciences, California, United States) at 4 °C until further use.

WJ-MSCs isolation and expansion

WJ tissues (n = 10) were trimmed, and small round segments were plated in 6-well plates (Costar, Corning Life, Canton, MA, United States) with 1 mL of standard culture medium in each well. The standard culture medium consisted of α-Minimum Essentials Medium (α-MEM, Gibco. Life Technologies, Grand Island, NY, United States) supplemented with 15% v/v Fetal Bovine Serum (Gibco. Life Technologies, Grand Island, NY, United States), 1% v/v Penicillin-Streptomycin (Gibco. Life Technologies, Grand Island, NY, United States) and 1% L-glutamine (Gibco. Life Technologies, Grand Island, NY, United States). Then, the plates were transferred in a humidified atmosphere with 5% CO_2 at 37°C, and left for 18 d. The standard culture medium was changed once per week. After 18 d, trypsinization of cells was performed using 0.025% Trypsin-EDTA (Gibco, Life Technologies, Grand Island, NY, United States) solution for 10 min at 37°C. The cells were replated in 75 cm^2 cell culture flasks (Costar, Corning Life, Canton, MA, United States). When confluency was observed (mostly after 10 d), the cells were trypsinized again and plated into 175 cm^2 cell culture flasks (Costar, Corning Life, Canton, MA, United States). The same procedure was repeated until cells reached P4.

Growth kinetics and cell viability of WJ-MSCs

The WJ-MSCs (n = 10) used in this study were evaluated for their total cell number, cell doubling time (CDT), cumulative population doubling (PD) and cell viability until reaching P4. WJ-MSCs were plated at a density of 2×10^5 cells in 75 cm^2 cell culture flasks (Costar, Corning Life, Canton, MA, United States), expanded and measured in each passage.

The CDT was calculated based on the following equation:

$$CDT = \log_{10}(N/N0) \div \log_{10}(2) \times T$$

The PD of each passage was determined with the following equation and added to the PD of the previous passages to obtain the cumulative PD.

The PD was estimated based on the equation:

$$PD = \log_{10}(N/N0) \div \log_{10}(2)$$

Where N was the number of cells at each passage, No was the number of initially plated WJ-MSCs and T was the culture duration in hours.

Total cell counting and viability estimations were performed using an automated system (Countess II FL Automated Cell Counter, Thermo Fischer Scientific, MA, United States) with Trypan blue stain (Invitrogen, ThermoFischer Scientific, MA, United States).

Additionally, cell viability was determined with Crystal Violet assays (ab232855, Abcam, Cambridge, United Kingdom) according to the manufacturer's instructions. Briefly, 2×10^5 MSCs from passages 1 to 4 were added to each well of a 96-well plate (Costar, Corning Life, Canton, MA, United States). DMSO vehicle was used as a background control, and doxorubicin was added in a well containing MSCs as a proliferation inhibitor. All MSC samples were cultured for 72 h at 5% CO_2 in a humidified atmosphere. Then, the culture medium was removed, cultures were washed and 50 μL of Crystal Violet was added to each well for 20 min at room temperature. Then, washing was performed and repeated four times, the 96-well plate was air dried, followed by the addition of 100 μL solubilization solution to each well. Finally, absorbance at 595 nm was measured, and the % cytotoxicity was calculated

based on the determination of the optical density (OD) using the following equation:

% Cytotoxicity = [OD (DMSO) – OD (Sample)] ÷ OD (DMSO) × 100%

Where OD (DMSO) was the DMSO control after background correction and OD (Sample) was the OD of the sample after background correction.

WJ-MSCs trilineage differentiation assay

WJ-MSCs P4 (n = 5) were promoted to differentiate towards "osteocytes", "adipocytes" and "chondrocytes". For "osteogenic" and "adipogenic" differentiation, WJ-MSCs were plated at a density of 1 × 10^5 cells into 6-well plates (Costar, Corning Life, Canton, MA, United States). When the cells reached 80% confluency, differentiation was performed. WJ-MSCs were differentiated into "osteocytes" or "adipocytes" using the STEMPRO® Osteogenesis (ThermoFischer Scientific, Massachusetts, United States) or STEMPRO® Adipogenesis (ThermoFischer Scientific, Massachusetts, United States) Differentiation kits, according to the manufacturer's instructions. Evaluation of "osteogenic" or "adipogenic" differentiation was conducted with the Alizarin Red S (Sigma-Aldrich, Darmstadt, Germany) and Oil Red-O (Sigma-Aldrich, Darmstadt, Germany) histological stains, respectively. Alizarin Red S specifically stains calcium depositions, while Oil-Red-O stains produced lipid droplets. In addition, Alizarin Red S quantification assays (ECM815, Millipore, Darmstadt, Germany) were used to determine Ca^{2+} deposits, according to the manufacturer's instructions. "Chondrogenic" differentiation was performed in 3D cultures generated from seeded WJ-MSCs at a density of 5 × 10^5 cells in 15 mL polypropylene falcon tubes (BD Biosciences, CA, United States). Then, 2 mL of chondrogenic differentiation medium was added to each 3D culture. Then, 3D cultures were placed in a humidified atmosphere with 5% CO_2 at 37°C for 4 wk. The chondrogenic differentiation medium consisted of high glucose D-MEM (Sigma-Aldrich, Darmstadt, Germany) supplemented with 0.01 mmol dexamethasone (StemCell technologies, Vancouver, BC, Canada), 40 g/mL ascorbic acid-2 phosphate (StemCell Technologies, Vancouver, BC, Canada), 10 ng/mL transforming growth factor-β1 (TGF-β1, Sigma-Aldrich, Darmstadt, Germany), and 100 μL of insulin-transferin selenium liquid medium 100× (ITS 100×, StemCell technologies, Vancouver, BC, Canada). After 4 wk of differentiation, 3D cultures were fixed with 10% v/v neutral formalin buffer (Sigma-Aldrich, Darmstadt, Germany), dehydrated, paraffin-embedded and sectioned into 5 μm slices. "Chondrogenic" induction of WJ-MSCs was evaluated with Alcian blue (Sigma-Aldrich, Darmstadt, Germany) staining, which is specific for cartilage proteoglycans.

Furthermore, chondrogenic differentiation was further assessed with the Bern Score. Specifically, three independent observers evaluated chondrogenic differentiation based on a previously published protocol[31].

Immunophenotypic analysis

Immunophenotypic analysis was performed in WJ-MSCs (n = 3) P4 as has been proposed by ISCT. Specifically, WJ-MSCs were analyzed for the expression of CD90 (Thy-1), CD105 (endoglin), CD73 (ecto-5′ nucleotidase), CD29 (integrin subunit), CD19 (pan-B-cell marker), CD31 (pan-EC marker), CD45 (pan-hematopoietic cell marker), CD34 (hematopoietic stem cell marker), CD14 (TLR-4 co-receptor), CD3 (T-cell co-receptor), HLA-DR (HLA class II antigen) and HLA-ABC (HLA class I antigen). Monoclonal antibodies against CD90, HLA-ABC, CD29, CD19, CD31 and CD45 were conjugated with fluorescein isothiocyanate (FITC), while CD105, CD73, CD44, CD3, CD34 and HLA-DR were conjugated with phycoerythrin. All monoclonal antibodies were purchased from Immunotech (Immunotech, Beckman Coulter, Marseille, France). Immunophenotypic analysis was performed with a Cytomics FC 500 flow cytometer (Beckman Coulter, Marseille, France), coupled with CXP Analysis software (Beckman Coulter, Marseille, France).

VSMCs differentiation protocol

WJ-MSCs P3 (n = 5) were used for differentiation into VSMCs. Specifically, 75 × 10^5 cells were seeded into 75 cm^2 cell culture flasks (Costar, Corning Life, Canton, MA, United States) until they reached 80% confluency. Then, brief washes with PBS 1× (Sigma-Aldrich, Darmstadt, Germany) were performed. After the total removal of the remaining buffer, WJ-MSCs were cultivated in DMEM high glucose (Gibco. Life Technologies, Grand Island, NY, United States) with 20% v/v UCB-PL and 30 μmol ascorbic acid (Sigma-Aldrich, Darmstadt, Germany) for a time period of 3 wk. The above medium will be referred to as VSMC differentiation medium, and was changed biweekly. The PL was produced from UCB units that did not meet the criteria for hematopoietic stem cell isolation of the Hellenic Cord Blood Bank, and the whole procedure was performed as has been previously reported[29]. WJ-MSCs P3 (n = 3) cultured with the standard culture medium served as negative controls in this study.

Gene expression profiling

Gene expression profiling of differentiated VSMCs was performed with reverse transcription polymerase chain reaction (PCR), followed by PCR and gel electrophoresis. Total mRNA was isolated from VSMCs (n = 5) using the TRI-reagent (Sigma-Aldrich, Darmstadt, Germany) according to the manufacturer's instructions. Quantity and quality of the isolated mRNA were determined photometrically. Then, 800 ng of total mRNA was transcribed into DNA using the Omniscript reverse transcription kit (Qiagen, Hilden, Germany). PCR was performed with Taq PCR Master Mix (Cat No 201443, Qiagen, Hilden, Germany) on a Biometra T Gradient Thermoblock PCR Thermocycler (Biometra, Gottingen, Germany). The final volume of each PCR reaction was 20 μL.

The amplification program used in the current study involved the following steps: initial denaturation at 95°C for 15 min, denaturation at 94°C for 30 s, annealing at 60-62°C for 90 s and final extension at 72°C for 3 min. A total of 35 cycles was used for the amplification of genomic DNA. The specific primers used for the current assay are listed in Table 1. All PCR products were analyzed by electrophoresis on a 1% w/v agarose gel (Sigma-Aldrich, Darmstadt, Germany). Finally, comparison of gene expression of differentiated VSMCs with undifferentiated WJ-MSCs (n = 5, negative control group) was performed. For gene expression profiling, the following genes were evaluated: *ACTA2, MYH11, TGLN, MYOCD, SOX9, NANOG, OCT4*, and *GAPDH*.

Immunofluorescence of VSMCs

Indirect immunofluorescence against ACTA2 and MYH11 was performed on WJ-MSCs (n = 5) and VSMCs (n = 5). Specifically, WJ-MSCs and VSMCs were seeded at a density of 1 × 10^4 cells on culture slides (Sigma-Aldrich, Darmstadt, Germany) for 48 h. Then, the cells were washed for 1-2 min with PBS 1× (Gibco. Life Technologies, Grand Island, NY, United States) and fixed for 5 min with 10% v/v neutral formalin buffer (Sigma-Aldrich, Darmstadt, Germany). The next step of the assay involved antigen retrieval and blocking of all samples, followed by the addition of monoclonal antibody against human ACTA2 (1:500, Catalog MA1-744, ThermoFischer Scientific, Massachusetts, United States) and MYH11 (1:1000, Catalog MA5-11971, ThermoFischer Scientific, MA, United States). Secondary FITC-conjugated rabbit IgG antibody (1:100, Sigma-Aldrich, Darmstadt, Germany) was added. Finally, DAPI (Sigma-Aldrich, Darmstadt, Germany) stain was added in order for the cell nuclei to become evident, and slides were glycerol mounted. Images were acquired using a LEICA SP5 II fluorescent microscope equipped with LAS Suite v2 software (Leica, Microsystems, Wetzlar, Germany). Furthermore, mean fluorescence intensity of WJ-MSCs and VSMCs was determined using ImageJ 1.46r (Wane Rasband, National Institutes of Health, United States).

Estimation of cell proliferation using ATP assay

Cell proliferation was determined with an ATP assay (MAK190, Sigma-Aldrich, Darmstadt, Germany) according to the manufacturer's instructions. Briefly, 1 × 10^5 WJ-MSCs or VSMCs were plated in 24-well plates (Costar, Corning Life, Canton, MA, United States). The next day, cells were lysed with 100 μL ATP assay buffer. Then, 20 μL of cell lysates were transferred to 96-well plates, followed by the addition of reaction buffer. All samples were incubated for 30 min at room temperature. Finally, the absorbance was measured by a photometer at 570 nm. Determination of ATP concentration was achieved by interpolation to a standard curve. The standard curve consisted of 0 (blank), 5, 10, 20, 50, 100, 150, and 200 nmol standards.

Decellularization of hUAs

The hUAs (n = 10, l = 2 cm) were immediately decellularized after their isolation from hUCs. Briefly, the hUAs were placed in CHAPS buffer (8 mmol CHAPS, 1 mol NaCl and 25 mmol EDTA in PBS 1×, Sigma-Aldrich, Darmstadt, Germany) for 22 h under rotational agitation. Furthermore, hUAs were transferred into SDS buffer (1.2 mmol SDS, 1 mol NaCl and 25 mmol EDTA in PBS 1×, Sigma-Aldrich, Darmstadt, Germany) for another 22 h under rotational agitation. Finally, the vessels were incubated in α-MEM with 40% v/v Fetal Bovine Serum (Sigma-Aldrich, Darmstadt, Germany) at 37°C for 48 h.

Histological analysis of hUAs

The efficacy of the decellularization protocol was evaluated by performing the following histological stains. Non-decellularized (n = 10, l = 2 cm) and decellularized (n = 10, l = 2 cm) hUAs were initially fixed with 10% v/v neutral formalin buffer (Sigma-Aldrich, Darmstadt, Germany), dehydrated, paraffin-embedded and sectioned into 5 μm slices. Hematoxylin and Eosin (H & E, Sigma-Aldrich, Darmstadt,

Table 1 Primer sets for polymerase chain reaction

Gene	Accession number	Forward primer	Reverse primer	Amplicon size
ACTA2	NM_001613	CAGCCAAGCACTGTCAGGAAT	CACCATCACCCCCTGATGTC	182
MYOCD	NM_001146312	CCACCTATGGACTCAGCCTAC	CTCAGTGGCGTTGAAGAAGAG	188
MYH11	NM_022844	CGCCAAGAGACTCGTCTGG	TCTTTCCCAACCGTGACCTTC	129
TGLN	NM_003564	ATGGCACGGTGCTATGTGAG	CCCACCCAGATTCATCAGCG	71
SOX9	NM_000346	AGCGAACGCACATCAAGAC	CTGTAGGCGATCTGTTGGGG	85
NANOG	NM_024865	TTTGTGGGCCTGAAGAAAACT	AGGGCTGTCCTGAATAAGCAG	116
OCT4	NM_001159542	GTGTTCAGCCAAAAGACCATCT	GGCCTGCATGAGGGTTTCT	156
GAPDH	NM_001256799	GGAGCGAGATCCCTCCAAAAT	GGCTGTTGTCATACTTCTCATGG	197

Germany), Sirius Red (SR, Sigma-Aldrich, Darmstadt, Germany) and Toluidine blue (TB, Fluka, Sigma-Aldrich, Darmstadt, Germany) were applied for the evaluation of cell and nuclear remnants, collagen and proteoglycan preservation in hUAs, respectively. Images were acquired using a Leica DM L2 light microscope (Leica Microsystems, Weltzar, Germany) and processed with ImageJ 1.46r (Wane Rasband, National Institutes of Health, United States).

In addition, indirect immunofluorescence against ACTA2 and MYH11 in combination with DAPI staining was applied. Non-decellularized and decellularized hUAs were fixed with 10% v/v formalin buffer (Sigma-Aldrich, Darmstadt, Germany), dehydrated, blocked and sectioned into 5 μm slices. Then, the slides were deparaffinized, rehydrated and blocked, followed by the addition of the monoclonal antibody ACTA2 (1:500, Catalog MA1-744, ThermoFischer Scientific, MA, United States) or MYH11 (1:1000, Catalog MA5-11971, ThermoFischer Scientific, Massachusetts, United States). Secondary FITC conjugated antibody (1:100, Sigma-Aldrich, Darmstadt, Germany) was added. Finally, DAPI (Sigma-Aldrich, Darmstadt, Germany) stain was added, the slides were glycerol mounted and processed for examination under the fluorescent microscope (LEICA SP5 II fluorescent microscope, Leica, Microsystems, Wetzlar, Germany).

Biochemical analysis

Evaluation of the decellularization procedure involved the quantification of collagen, sulphated glycosaminoglycans and DNA of non-decellularized (n = 10, l = 2 cm) and decellularized dry tissue samples (n = 10, l = 2 cm). Quantification of collagen was performed based on the measurement of hydroxyproline content, and relied on the use of the Hydroxyproline Assay Kit (MAK008, Sigma-Aldrich, Darmstadt, Germany) according to the manufacturer's instructions. Quantification of sGAGs initially involved the digestion of samples in 125 μg/mL papain buffer at 60°C for 12 h, followed by the addition of dimethylene blue dye (Sigma-Aldrich, Darmstadt, Germany). The concentration of sGAGs in each sample was estimated through interpolation to a standard curve. Chondroitin sulphate standards of 12 μg/mL, 25 μg/mL, 50 μg/mL, 100 μg/mL and 150 μg/mL were used for the standard curve.

DNA content was estimated in non-decellularized (n = 10, l = 2 cm) and decellularized (n = 10, l = 2 cm) hUAs after their digestion in lysis buffer. Lysis buffer contained 0.1 mol Tris pH 8, 0.2 mol NaCl, 5 mmol EDTA in PBS 1× supplemented with 20 mg/mL Proteinase K (Sigma-Aldrich, Darmstadt, Germany). Total DNA of each sample was isolated, eluted in 100 μL DNAse-free water (Sigma-Aldrich, Darmstadt, Germany) and photometrically quantified at 260 nm to 280 nm.

Repopulation of hUAs with VSMCs

Decellularized hUAs (n = 30, l = 1 cm) were repopulated with VSMCs under static seeding conditions. For this purpose, decellularized hUAs were placed into 24-well plates (Costar, Corning Life, Canton, MA, United States) with VSMCs at an average number of 3×10^5 cells. Then, 1 mL of VSMC differentiation medium was carefully added in each well. The plates were transferred to a humidified atmosphere with 5% CO_2 at 37°C for 3 wk. After the proposed time period, evaluation of the repopulation results was performed with H & E, in the same way as referred to in the previous sections (Histological analysis). In addition, indirect immunofluorescence against MYH11 in combination with DAPI staining was applied. Repopulated hUAs with VSMCs were fixed with 10% v/v formalin buffer (Sigma-Aldrich, Darmstadt, Germany), dehydrated, blocked and sectioned into 5 μm slices. Then, the slides were deparaffinized, rehydrated and blocked, followed by the addition of monoclonal antibody against MYH11 (1:1000, Catalog MA5-11971, ThermoFischer Scientific,

Massachusetts, United States). Secondary FITC conjugated antibody (1:100, Sigma-Aldrich, Darmstadt, Germany) was added. Finally, DAPI (Sigma-Aldrich, Darmstadt, Germany) stain was added, the slides were glycerol mounted and processed for examination under a fluorescent microscope (LEICA SP5 II fluorescent microscope, Leica, Microsystems, Wetzlar, Germany).

In addition, immunohistochemistry against Ki67 and proliferating cell nuclear antigen (PCNA) was performed on the repopulated hUAs. Briefly, the slides were deparafinized, rehydrated and the whole procedure was performed using the Envision Flex Mini Kit, high pH (Cat # K802421-2J, Agilent Technologies, CA, United States) according to the manufacturer's instructions. Ki67 (1:50, Cat # 305504, Biolegend, San Diego, United States) and PCNA (1:100, ab 18197, Abcam, Cambridge, United Kingdom) were used for the detection of cell proliferation in the repopulated hUAs. Decellularized hUAs served as a negative control both in the indirect immunofluorescence and immunohistochemistry assays. Furthermore, hydroxyproline and sGAG contents were quantified in the repopulated hUAs (n = 20) in the same way as referred to in the previous section (Biochemical Analysis). Decellularized hUAs (n = 20) served as the negative control group. Finally, VSMC proliferation in the repopulated hUAs was further confirmed and assessed by DNA quantification. HUAs were digested with lysis buffer as referred to previously (Biochemical Analysis), and the DNA amount was quantified photometrically at 260 nm to 280 nm.

Determination of ATP-ADP Ratio in repopulated hUAs

The evaluation of VSMC viability in repopulated hUAs was performed with an ADP/ATP assay kit (MAK189, Sigma -Aldrich, Darmstadt, Germany) according to the manufacturer's instructions. Briefly, the light intensity, which is specific to intracellular ATP concentration, is produced with the following reaction:

ATP + D-Luciferin + O_2 → oxyluciferin + AMP + PP_i + CO_2 + light

In the next step, the ADP is converted to ATP, which further reacts with D luciferin. The second light intensity determines the total ADP and ATP concentration. The light intensity was measured using a luminometer (Lucy 1, Anthos, Luminoskan, Labsystems) and expressed as the number of relative light units (RLUs). The determination of ADP/ATP ratio is performed using the following formula:

ADP/ATP ratio = (RLU C – RLU B) ÷ RLC A

Where RLU A is the initial luminescence measurement after the addition of the ATP reagent. RLU B is the luminescence measurement after 10 min of incubation, and RLU C is the measurement of light intensity after the addition of ADP reagent.

Briefly, decellularized hUAs (n = 10) were digested with collagenase IV (Sigma-Aldrich, Darmstadt, Germany), and the lysates were supplemented with a-MEM. In addition, VSMCs at a density of 2 × 10^5 cells were seeded in 24-well plates with 1 mL of decellularized hUA lysates. Finally, cell cultures were incubated for a total of 7 d in a humidified atmosphere and 5% CO_2. VSMCs with 10% v/v DMSO were used as a positive control group, while VSMCs with non-decellularized hUAs served as a negative control group for this study. The determination of ADP/ATP ratio was performed at the end of each day.

Statistical analysis

GraphPad prism v 6.01 (GraphPad Software, San Diego, CA, United States) was used for statistical analysis. Comparison of collagen, sGAG and DNA content between samples was performed using Kruskal Wallis and Mann Whitney tests. Statistically significant difference was considered when the P value was less than 0.05. Indicated values were presented as mean ± SD.

RESULTS

Characteristics of isolated WJ-MSCs

WJ-MSCs were successfully isolated and expanded from hUCs. Specifically, spindle-shaped cells were isolated from all samples. Furthermore, WJ-MSCs retained their morphological features until P4 (Figure 1A). To better determine the WJ-MSCs characteristics, total cell number, CDT, cumulative PD and cell viability were measured. Total cell number of WJ-MSCs at P4 surpassed 12 × 10^6 cells (Figure 1B). CDT and cumulative PD at P4 were 36 ± 3 h and 6 ± 1, respectively (Figure 1C and D). Cell viability of WJ-MSCs, determined either with Trypan blue or Crystal Violet in passages 1 to 4, was above 90% (Figure 1E and Supplementary Figure 1).

WJ-MSCs of P4 successfully differentiated towards "osteogenic", "adipogenic" and "chondrogenic" lineages, as indicated by the histological stains (Figure 1F).

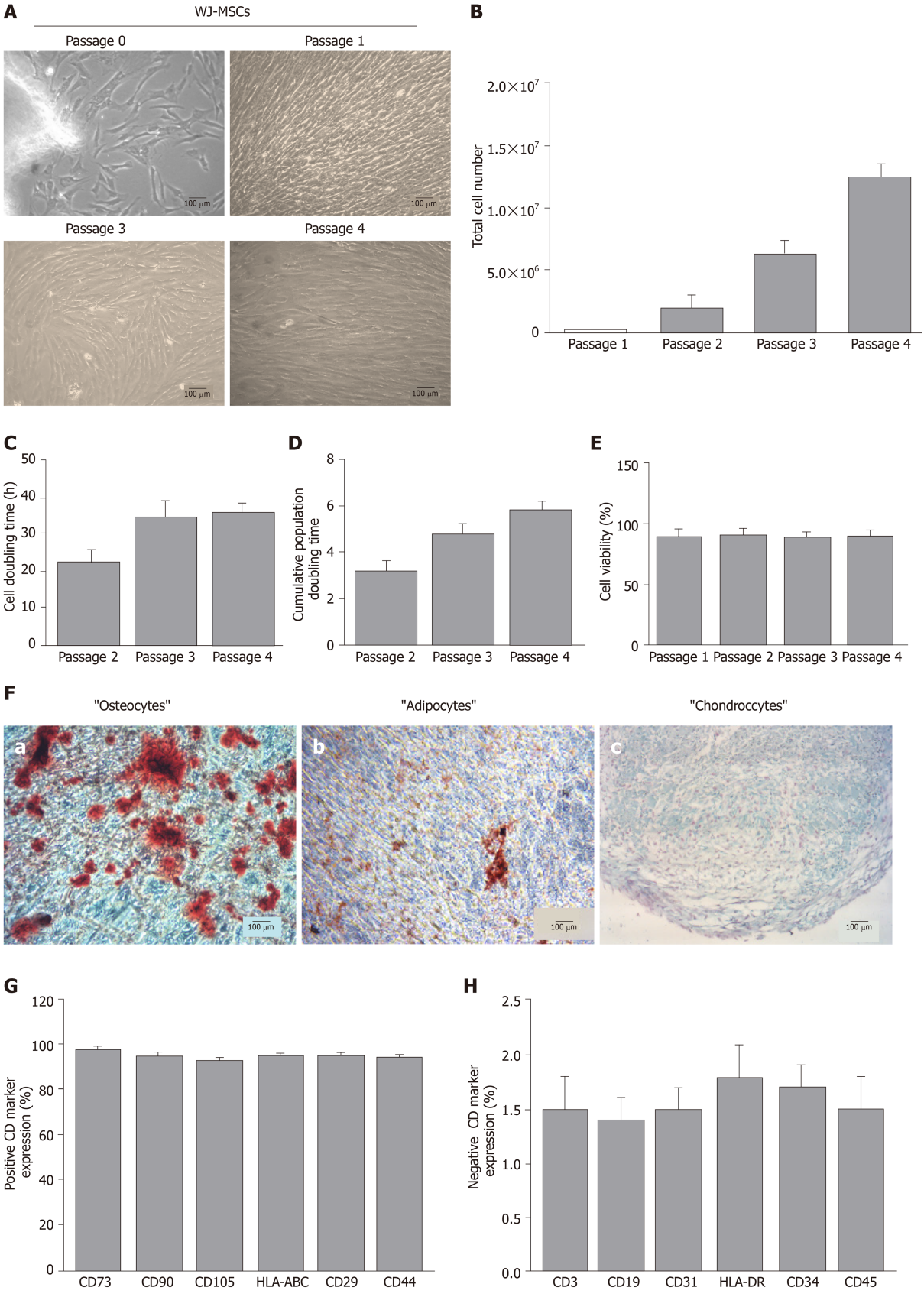

Figure 1 Evaluation of mesenchymal stromal cells derived from the Wharton's Jelly. A: Morphological features of mesenchymal stromal cells derived from the Wharton's Jelly tissue (WJ-MSCs) from P0 to P4 (A-a to A-d); B-F: Determination of total cell number (B), cell doubling time (C), cumulative PD (D) and cell viability (E) of WJ-MSCs from P0 to P4. Evaluation of tri-lineage differentiation capability of WJ-MSCs into "osteocytes" (F-a), "adipocytes" (F-b) and "chondrocytes" (F-c) as indicated by Alizarin Red-S, Oil-Red-O and Alcian blue, respectively. G, H: Positive (G) and negative (H) expression of CD markers in WJ-MSCs based on flow cytometric analysis. Images A-a to A-d and F-a to F-c were obtained with original magnification 10× and 100 μm scale bars. WJ-MSCs: Mesenchymal stromal cells derived from the Wharton's Jelly tissue.

Specifically, after 4 wk of "osteogenic" differentiation conditions, cells were characterized by calcium deposits, which stained red with Alizarin Red S (Figure 1F). Moreover, "osteocytes" produced Ca^{2+} deposits more than 0.9 mmol (Supplementary Figure 2). Under "adipogenic"-inducing conditions, WJ-MSCs successfully produced lipid vacuoles, which were visible with Oil Red O staining (Figure 1F). In regards to "chondrogenic" differentiation, 3D cultures of WJ-MSCs were characterized by the production of proteoglycan aggregations, as was indicated by Alcian blue and Bern Scores (Figure 1F and Supplementary Table 1). Flow cytometry analysis showed that WJ-MSCs were characterized by their positive expression of up to 92% for CD73, CD90, CD105, CD29, HLA-ABC and CD44, and by their negative expression below 2% for CD3, CD19, CD31, HLA-DR, CD34 and CD45 (Figure 1G and 1H).

Evaluation of VSMC differentiation

WJ-MSCs were successfully differentiated into VSMCs with the proposed differentiation protocol. Treatment of WJ-MSCs with UCB-PL in combination with ascorbic acid resulted in cells with more elongated spindle-shaped morphologies compared with undifferentiated cells (Figure 2A). VSMC markers such as *ACTA2, MYOCD, MYH11* and *TGLN* were expressed at the mRNA level in differentiated cells (Figure 2B). In addition, differentiated VSMCs also expressed *SOX9* (Figure 2B). Pluripotency-related genes, such as *NANOG* and *OCT4*, were not expressed in differentiated VSMCs (Figure 2B). On the other hand, untreated WJ-MSCs did not express the above markers, with the only exception being *ACTA2* (Figure 2B). WJ-MSCs successfully expressed pluripotency-related genes such as *NANOG* and *OCT4* (Figure 2B).

The estimation of WJ-MSC and VSMC proliferation was performed using the ATP assay. Both cellular populations were characterized by equal amounts (17 ± 3 nmol and 18 ± 3 nmol) of ATP (Figure 2C).

Further determination of successful VSMC differentiation involved the performance of indirect immunofluorescence against ACTA2 and MYH11 in combination with DAPI stain (Figure 2D and Supplementary Figure 3). Early and late VSMC-specific genes such as ACTA2 and MYH11 were successfully expressed after 3 wk (Figure 2D and Supplementary Figure 3). Untreated WJ-MSCs were characterized by low expression of ACTA2, while totally lacked MYH11 expression (Figure 2D and S3).

In addition, mean fluorescence intensity of ACTA2 and MYH11 was determined in both WJ-MSCs and VSMCs (Supplementary Figure 4). Statistically significant differences were observed in the ACTA2 ($P < 0.01$) and MYH11 ($P < 0.01$) expression levels of WJ-MSCs and VSMCs (Supplementary Figure 4), indicating the successful differentiation of VSMCs. The above results were in accordance with gene expression analysis, demonstrating the differentiation efficiency.

Decellularization of hUAs

HUAs were successfully decellularized as showed by histological analysis. Decellularized hUAs were characterized by intact ECM, without any cellular or nuclear remnants (Figure 3A). In addition, key specific ECM components, such as collagen and sGAGs, seemed to be preserved according to SR and TB stains, respectively (Figure 3A). SR stains showed that the collagen structure and orientation was preserved (Figure 3A). In addition, TB stains appeared to be less dense in decellularized hUAs compared to non-decellularized vessels. Signal detection of ACTA2, MYH11 and DAPI was evident only in non-decellularized hUAs, confirming the successful decellularization procedure (Figure 3A).

Further evaluation of the decellularization procedure in hUAs involved biochemical analysis, which included the determination of collagen (hydroxyproline), sGAG and DNA contents. Specifically, hydroxyproline content in native hUAs was 93 ± 12 μg hydroxyproline/mg of dry tissue weight, while in decellularized hUAs was 72 ± 10 μg hydroxyproline/mg of dry tissue weight (Figure 3B). Statistically significant differences in hydroxyproline content was observed between non-decellularized and decellularized hUAs ($P < 0.001$). SGAG content was significantly ($P < 0.001$) lower in decellularized hUAs compared to non-decellularized hUAs (Figure 3C). SGAG content in non-decellularized and decellularized hUAs was 5 ± 1 and 2 ± 1 μg sGAG/mg of dry tissue weight (Figure 3C). DNA content was totally eliminated in decellularized hUAs, further confirming the histological results. DNA content in non-decellularized hUAs was 1503 ± 120 ng DNA/ mg of dry tissue weight, and in decellularized hUAs was 41 ± 6 ng DNA/mg of dry tissue weight (Figure 3D). Statistically significant differences were observed in DNA content between non-decellularized and decellularized hUAs ($P < 0.001$).

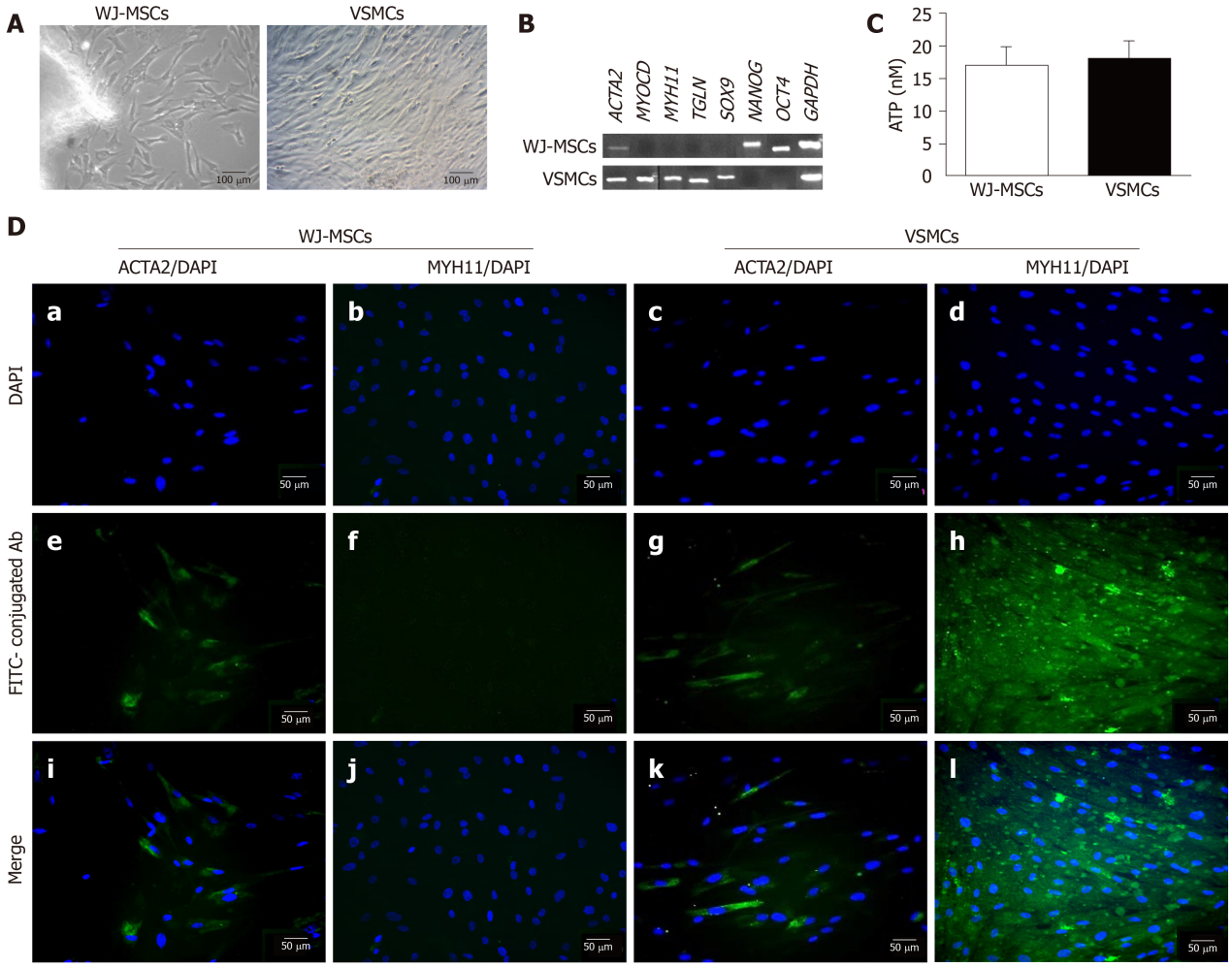

Figure 2 Differentiation of mesenchymal stromal cells derived from the Wharton's Jelly tissue into vascular smooth muscle cells. A: Morphological features of untreated mesenchymal stromal cells derived from the Wharton's Jelly tissue (WJ-MSCs) and differentiated vascular smooth muscle cells (VSMCs); B: Polymerase chain reaction results regarding the expression of VSMC-specific genes, such as *ACTA2, MYOCD, MYH11* and *TGLN*, and pluripotency-related genes, including *NANOG* and *OCT4* in untreated WJ-MSCs and differentiated VSMCs. *GAPDH* was the desired house-keeping gene for current analysis; C: Determination of WJ-MSC and VSMC proliferation by performing the ATP assay; Indirect immunofluorescence against the early VSMC marker ACTA2 and late VSMC marker MYH11 in untreated WJ-MSCs (D-a, D-e, D-i and D-b, D-f, D-j) and differentiated VSMCs (D-c, D-g, D-k and D-d, D-h, D-l) in combination with DAPI, respectively. Images A-a and A-b were presented with 10× original magnification and 100 μm scale bars. Images D-a to D-l were presented with 20× original magnification and 50 μm scale bars. WJ-MSCs: Mesenchymal stromal cells derived from the Wharton's Jelly tissue; VSMCs: Vascular smooth muscle cells.

Repopulation of hUAs with VSMCs

Decellularized hUAs were successfully repopulated by VSMCs under static seeding conditions. Indeed, VSMCs appeared in the outer layer of the vessels from the 1st wk of seeding (Figure 4A and Supplementary Figure 5). These cells were successfully expanded on vessel walls after 3 wk of repopulation (Figure 4A and Supplementary Figure 5). Indirect immunofluorescence results showed the presence of differentiated VSMCs in the outer surface of decellularized vessels, further confirming the H & E results. In addition, immunohistochemistry results indicated the expression of key proliferation markers such as Ki67 and PCNA in the VSMCs of repopulated hUAs (Figure 4A).

Further evaluation of the repopulated arteries involved the quantification of hydroxyproline and sGAG content. Specifically, total hydroxyproline content after the 1st, 2nd and 3rd wk was 71 ± 10, 74 ± 9 and 86 ± 8 μg hydroxyproline/mg of dry tissue weight, respectively (Figure 4B). Overall, total hydroxyproline content appeared to be increased within the first week of repopulation. Statistically significant differences in total hydroxyproline content were observed between the study groups ($P < 0.05$). SGAG content of the 1st, 2nd and 3rd wk was 2 ± 1, 3 ± 1 and 3 ± 1 μg sGAG/mg of dry tissue weight, respectively (Figure 4C). Statistically significant differences were observed between the study groups ($P < 0.05$). VSMCs exhibited robust proliferation in the hUAs, as was indicated by the DNA quantification results. Specifically, the DNA amount of repopulated hUAs after the 1st, 2nd and 3rd wk was 110 ± 21, 360 ± 61 and 554 ± 49 ng DNA/mg of dry tissue weight, while decellularized hUAs were

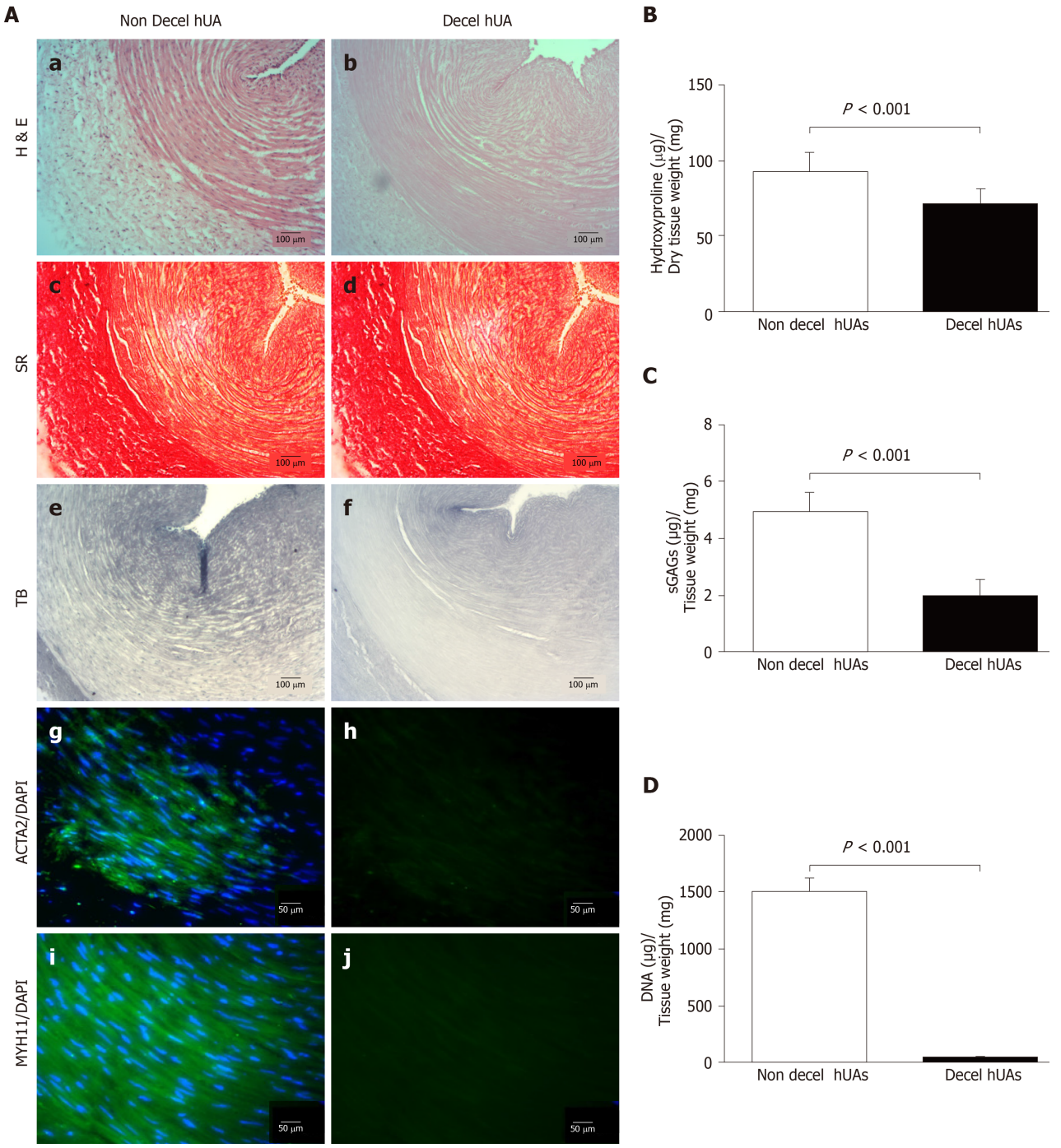

Figure 3 Histological and biochemical analysis of decellularized human umbilical arteries. A: Histological analysis with H & E (A-a, A-b), SR (A-c, A-d) and TB (A-e, A-f) in non-decellularized and decellularized human umbilical arteries (hUAs). Indirect immunofluorescence against ACTA2 (A-g, A-h) and MYH11 (A9,10) in combination with DAPI was performed in non-decellularized and decellularized hUAs; B-D: Biochemical analysis involved the determination of total hydroxyproline (B), sGAG (C) and DNA content (D) in non-decellularized and decellularized hUAs. Statistically significant differences were observed in total hydroxyproline ($P < 0.05$), sGAG ($P < 0.001$) and DNA ($P < 0.001$) content between non decellularized and decellularized hUAs. Images A-a to A-f were presented with original magnification 10× and 100 μm scale bars. Images A-g to A-j were presented with original magnification 20× and 50 μm scale bars. Non Decel hUA: Non decellularized human umbilical artery; Decell hUA: Decellularized human umbilical artery.

characterized by only 38 ± 7 ng DNA/mg of dry tissue weight (Figure 4D). Statistically significant differences were observed between the study groups ($P < 0.001$). No sign of any cytotoxic effects during VSMC proliferation in hUAs was observed, according to the determination of the ADP/ATP ratio (Figure 4E).

DISCUSSION

The development of well-defined VSMCs, which can be applied to the development

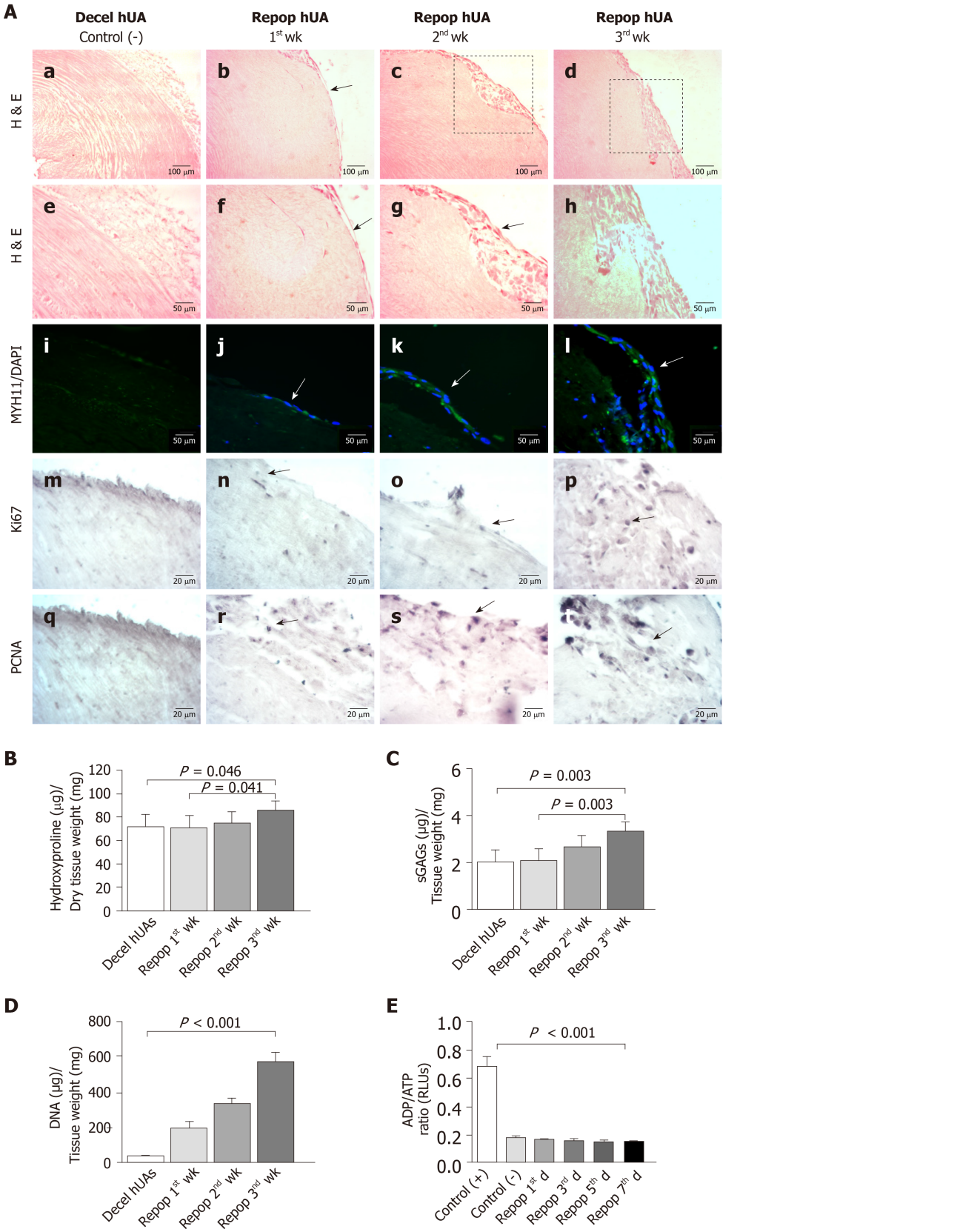

Figure 4 Repopulation of decellularized human umbilical arteries with vascular smooth muscle cells. A: Histological analysis with H & E of decellularized human umbilical arteries (hUAs) (A-a, A-e), repopulated hUAs after 1st wk (A-b, A-f), 2nd wk (A-c, A-g) and 3rd wk (A-d, A-h). Indirect immunofluorescence against MYH11 in combination with DAPI of decellularized hUAs (A-i), repopulated hUAs after 1st wk (A-j), 2nd wk (A-k) and 3rd wk (A-l). Immunohistochemistry against Ki67 and PCNA of decellularized hUAs (A-m, A-q), and repopulated hUAs after 1st wk (A-n, A-r), 2nd wk (A-o, A-s) and 3rd wk (A-p, A-t). Images A-a to d were presented with original magnification 10×, 100 μm scale bars. Images A-f to l were presented with original magnification 20× and 50 μm scale bars. Images A-i to t were presented with original magnification 40× and 20 μm scale bars; B, C: Total hydroxyproline (B) and sGAG (C) quantification of hUAs before and after repopulation with VSMCs; D, E: Determination of DNA content (D) and ADP/ATP ratio (E). Statistically significant differences in total hydroxyproline, sGAG, DNA content and ADP/ATP ratio were observed between the study groups ($P < 0.05$). Decel hUA: decellularized human umbilical artery, repop hUA: repopulated human umbilical artery.

of vascular grafts, is one of the major goals of blood vessel engineering. In order to obtain VSMCs, several sources of stem cells can be used. Unlike other stem cells, MSCs can be easily isolated from various human tissues such as bone marrow, adipose tissue and WJ tissue, and can be characterized by low immune responses, high proliferation rates and low risk of genome instability[32]. The aim of this study was the development of VSMCs through a differentiation process utilizing WJ-MSCs, for future use in small diameter vascular graft engineering.

Within this scope, WJ-MSCs were successfully isolated and expanded from WJ tissue until they reached P4. WJ-MSCs retained their spindle-shaped morphology through passages, and were characterized by high proliferation rates and cell viability. In addition, these cells were successfully differentiated into "osteocytes", "adipocytes" and "chondrocytes", as was confirmed by the presence of calcium deposits, lipid vacuoles and proteoglycan production. Immunophenotypic analysis provided evidence that WJ-MSCs positively expressed (> 90%) CD73, CD90, CD105, CD44 and CD29, while CD34, CD45, HLA-DR, CD3 and CD19 were negatively expressed (< 3%). These results indicated that the WJ-MSCs used in this study were a properly defined stem cell population, and fulfilled the minimum criteria defined by ISCT[30].

Once we established the properties of WJ-MSCs, they were then differentiated towards VSMCs. To promote the development of VSMCs from WJ-MSCs, a differentiation protocol that utilized the UCB-PL in combination with ascorbic acid was applied. UCB-PL contains significant amounts of growth factors such as TGF-β1, PDGF-A, FGF2, IFN-γ and TNF-α[29]. Among them, TGF-β1 and PDGF-A *via* their receptor are related to the activation of downstream SMADs and the MEK/ERK signaling pathway, contributing in this way to the differentiation process of VSMCs[23]. After 3 wk of differentiation, WJ-MSCs presented a more elongated spindle-shaped morphology. Moreover, these cells expressed *ACTA2, MYH11, MYOCD, TGLN* and *SOX9*. *ACTA2* is an early myogenic differentiation marker that is also expressed in WJ-MSCs. On the other hand, *MYH11, MYOCD* and *TGLN* are late myogenic differentiation markers that are especially expressed in VSMCs. Indeed, *MYH11* is required for the production of smooth-muscle myosin heavy chain, while *TGLN* is related to actin re-organization and shape change interactions[23]. *MYOCD* has a great role in the VSMC differentiation process, and its expression is restricted in smooth and cardiac muscle lineages[23]. MYOCD interacts with Serum Response Factor, thus forming a complex that binds to the CArG [CC(A/T)$_6$GG] box. CArG boxes are located in the promoters of SMC genes, regulating their transcription[32]. In our case, the myogenic differentiation conditions that were applied to WJ-MSCs induced the expression of *MYOCD*, which further regulates the transcription of contractile smooth muscle genes including *ACTA2*, *MYH11* and *TGLN*, thus promoting cell shape alterations[23,33]. Further clarification of the proper differentiation of VSMCs was provided by the indirect immunofluorescence assay against the early and late myogenic markers ACTA2 and MYH11. VSMCs were characterized by high expression of ACTA2 and MYH11, while untreated WJ-MSCs were characterized only by their low expression of ACTA2[34]. These results further confirmed our initial data at the mRNA level, indicating the successful differentiation of VSMCs. The low expression of ACTA2 in WJ-MSCs has been previously reported by other groups[35]. For this purpose, the MYH11 was used in order in our experimental approach to distinguish and characterize the differentiation state of WJ-MSCs. In addition, differentiated VSMCs expressed *SOX9*, a gene that is related to collagen production and the adaption of VSMC synthetic phenotypes[34]. *SOX9* expression may be relevant to the differentiation conditions that were applied in the current study. It is known that specific stress-strain conditions are required for the maintenance of contractile VSMC phenotypes[23]. In our study, no stress-strain conditions were applied, which may explain the *SOX9* expression in the differentiated VSMCs.

On the other hand, undifferentiated WJ-MSCs expressed only *OCT4* and *NANOG*. It is known that NANOG, in combination with other transcription factors such as OCT4, SOX2 and KLF4, establish the pluripotent state of stem cells[36]. These transcription factors block the Serum Response Factor association with CarG boxes, thus promoting *SMC* gene repression. VSMCs were not characterized by the expression of *OCT4* and *NANOG*. The repression of these genes might also contribute to the initiation of the differentiation process. Both WJ-MSCs and VSMCs were characterized by the equal production of ATP, suggesting the retention of VSMC proliferation properties.

Further work must be performed in order to obtain safer conclusions regarding the gene interplay during the VSMC differentiation process. The proposed differentiation protocol could induce the myogenic differentiation of WJ-MSCs utilizing only the exogenous supplementation of ascorbic acid. Our results seemed to be comparable with other previously published studies[37-43], where early, intermediate and late

VSMC markers such as ACTA2 and MYH11 are expressed. However, most of these studies apply more complicated and sophisticated approaches, including the use of iPSC technology, or the prolonged exogenous supplementation of growth factors[24-27]. Moreover, the use of iPSC technology in humans is under strict control. Modern research is focused on the production of safe viral-free iPSC clones for use in clinical trials. On the other hand, vascular tissue engineering demands a great number of cells, which are difficult to obtain from patients. Most of the time, vessel tissue biopsies are needed for the isolation of VSMCs. However, patient condition and age are important factors that may hamper VSMC isolation. In our study, the production of VSMCs from MSCs is proposed. MSCs can be efficiently isolated from several human patient tissues, including bone marrow and adipose tissue. Additionally, MSCs are pluripotent stem cells that can be expanded in great numbers, and can then be differentiated into the desired cell populations, such as VSMCs. Taken together, all these data propose an alternative way to obtain functional VSMCs, even from seriously diseased patients, for possible use in vascular tissue engineering.

The next step of this study was the use of VSMCs in small diameter vascular graft engineering. To date, several sources for the production of small diameter vascular grafts have been proposed, such as the use of Dacron and expanded polytetrafluorethylene conduits, and autologous vessels. Unlike these vessels, hUAs may possess an alternative source for the production of small diameter vascular grafts. In this way, hUAs were successfully decellularized as indicated by histological analysis. H & E staining revealed the preservation of ECM, without any cellular or nuclear remnants, while SR and TB showed the preservation of key ECM components such as collagen and sGAGs. Indirect immunofluorescence results indicated no presence of ACTA2 or MYH11 in decellularized hUAs, further confirming cell elimination. Biochemical analysis confirmed the presence of collagen and sGAGs, although both components were significantly reduced after the decellularization procedure. In addition, the DNA content of decellularized vascular grafts was significantly reduced, and was below 50 ng/mg of dry tissue as proposed by Crapo *et al*[44], thus further confirming the successful decellularization of hUAs. These results were in accordance with previously published studies conducted in vessels or other tissues, and the reduction of the above macromolecules were mostly attributed to SDS, a key reagent in the decellularization process[3,4,17,45]. However, hUA ECM was characterized as having the proper orientation of collagen and sGAGs, thus serving as an ideal vascular scaffold for cell repopulation.

Within this scope, the VSMCs were seeded on decellularized hUAs under static conditions. After the 1st wk of seeding, VSMCs were observed in the outer layer of the vessel. After 3 wk, the VSMCs appeared to expand onto the decellularized hUA, as was confirmed by H & E staining.

VSMCs were successfully characterized by MYH11 positivity, as indicated by immunofluorescence results after 3 wk of repopulation. Repopulated hUAs were also positive for Ki67 and PCNA, as was indicated by immunohistochemistry, confirming the successful proliferation of VSMCs. Also, an increase in DNA content was observed in repopulated hUAs, indicating the successful seeding and proliferation of VSMCs. Indeed, hUAs did not exhibit any cytotoxic effects, thus supporting the repopulation of VSMCs. For further evaluation of VSMC functionality, hydroxyproline and sGAG quantifications were performed. Total hydroxyproline content was increased even after the 1st wk of seeding. After 3 wk, the hydroxyproline content of the repopulated vessels was higher compared to the decellularized hUAs. In a similar way, sGAG content was higher in repopulated vessels after 3 wk compared to the decellularized hUAs. However, total hydroxyproline and sGAG content in repopulated hUAs was similar to the amount of native vessels. However, the further maturation of vessels is required through the use of other approaches, such as vessel bioreactors. Indeed, vessel bioreactors could contribute to a more uniform distribution of cells in vessel layers, thus inducing the proper maturation of vascular grafts, and likely the increase of total hydroxyproline and sGAG content[46].

Moreover, the above results confirmed that VSMCs retained their myogenic properties in the vascular scaffolds. Taking into consideration the expression of *SOX9* at the mRNA level in combination with the hydroxyproline production, it can be assumed that VSMCs retain their myogenic properties and contribute to the remodeling of vessel ECM. It is known that SOX9 in combination with RUNX2 and MSX2 could contribute to the synthetic conversion of VSMCs, resulting in collagen and sGAG synthesis. Although, in our study where only static seeding conditions were applied, the proper maturation of VSMCs and the adaption of contractile phenotypes onto decellularized vessels may require other approaches, such as the use of dynamic seeding conditions. Indeed, a pulsatile vessel bioreactor could mimic the blood flow of the human body with specific stress-strain conditions, and could contribute to the adaption of contractile phenotypes by VSMCs.

Future experiments will involve the use of a pulsatile vessel bioreactors for the repopulation approach in order to better define the VSMCs, and promote the maturation of vascular grafts. Moreover, a combination of VSMCs with EC is desired in order to produce fully functional small diameter vascular grafts.

In conclusion, in this study, VSMCs were successfully generated from WJ-MSCs and efficiently repopulated decellularized hUAs. Moreover, the differentiation of VSMCs relied on a protocol that utilized UCB-PL, excluding the exogenous supplementation of growth factors or ectopic expression of transcription factors[23]. Furthermore, the interaction of VSMCs *via* integrin connections such as $\alpha_v\beta_1$ with ECM proteins could maintain even more their a differentiation state. Until now, several complicated and expensive approaches are used for the production of vascular populations and small diameter vessel conduits[26,27,28,47]. Unlike these approaches, our proposal relied on the use of hUCs and their derivatives as an alternative approach for blood vessel engineering. From a material that is discarded after gestation, WJ-MSCs and hUAs can be efficiently isolated, while UCB-PL can be used for the production of myogenic differentiation medium.

The future goal will be the production and the proper maintenance of patient-specific small diameter vascular grafts under good manufacturing practice conditions, in order to be readily accessible upon demand.

ARTICLE HIGHLIGHTS

Research background

Small diameter vascular grafts can be applied in a wide variety of diseases, but mostly in cardiovascular disease (CAD). Globally, CAD affects more than 18 million people, and it is estimated that more than 500000 bypass surgeries are performed. Until now, autologous saphenous vein transplants, or conduits made of Dacron or ePTFE, represent the gold standard strategy. However, severe side effects, including impaired patency, immune reaction and intima hyperplasia, may be accompanied by their use. For this purpose, the decellularization of human umbilical arteries and the repopulation with vascular smooth muscle cells (VSMCs) in order to obtain fully functional vascular grafts, could represent an alternative approach. VSMCs are a cellular population responsible for vasoconstriction and vasodilation. Recently, the development of VSMCs has been proposed using induced pluripotent stem cell (iPSCs) technology. However, iPSCs have not been approved for broad human use. In this way, an alternative approach using platelet lysate from umbilical cord blood (UCB-PL) may be applied in the differentiation process of VSMCs from mesenchymal stromal cells (MSCs). It is known that UCB-PL contains significant amounts of growth factors such as TGF-β1, PDGFA, FGF2, IFN-γ and TNF-α, which have previously been used in several differentiation protocols. The aim of this study was to establish the differentiation process of VSMCs from MSCs derived from the Wharton's Jelly tissue (WJ-MSCs) using the UCB-PL. Then, the differentiated VSMCs were used for repopulation experiments of decellularized human umbilical arteries (hUAs) to produce fully functional small diameter vascular grafts.

Research motivation

Until now, the development of VSMCs is accomplished using exogenous supplementation of several growth factors or through iPSC technology. However, both approaches may cause allergic reactions or could even be tumorigenic. Indeed, a great number of growth factors are derived from animals. Additionally, iPSC technology has not received full approval from the Food and Drug Administration for human use, due to the use of c-Myc, which may lead to tumor development. In order to overcome these issues, the differentiation of VSMCs from MSCs using UCB-PL and ascorbic acid has been proposed. It has been shown in the past that specific growth factors, especially TGF-β1, could promote the differentiation of VSMCs. UCB-PL contains several growth factors, including TGF-β1, PDGF-A, FGF2, IFN-γ and TNF-α, and in combination with ascorbic acid may lead to the successful development of VSMCs.

Research objectives

The main objective of this study was the successful differentiation of VSMCs obtained from WJ-MSCs using UCB-PL. Secondary objectives were the production of small diameter vascular grafts in hUAs using the decellularization method. In addition, the repopulation of decellularized vessels with the produced VSMCs, which may result in functional vessels, was also evaluated in this study.

Research methods

Initially, WJ-MSCs were isolated from hUCs and expanded until they reached P4. Characterization of WJ-MSCs was performed according to the criteria of the International Society for Cell and Gene Therapy, including morphological evaluation, trilineage differentiation and flow cytometry analysis. Then, the differentiation of VSMCs was performed. To do this, WJ-MSCs were cultured in a medium containing UCB-PL and ascorbic acid for 3 wk. Gene expression profiles of VSMCs for *ACTA2, MYH11, TGLN, MYOCD, SOX9, NANOG, OCT4, and GAPDH* by RT-PCR, PCR and gel electrophoresis were evaluated. Further analysis included the indirect immunofluorescence of VSMCs using antibodies against ACTA2 and MYH11. The production of vascular grafts was performed using the decellularization of hUAs. Then

histological (H & E, SR and TB stains) and biochemical analyses (hydroxyproline, sGAG, DNA content) in decellurized hUAs were applied. Finally, the repopulation of decellularized hUAs with VSMCs through static seeding was performed. Repopulated vessels were analyzed histologically (H & E, MYH11/DAPI) and biochemically (hydroxyproline, DNA content and ADP/ATP ratio). In addition, the proliferation of VSMCs in repopulated vessels was immunohistochemically evaluated using Ki67 and proliferating cell nuclear antigen.

Research results

WJ-MSCs were successfully isolated and expanded from hUCs. Their spindle-shaped morphology was retained until they reached P4. Total cell number, CDT and PD of WJ-MSCs at P4 was > 12×10^6 cells, 36 ± 3 h and 6 ± 1, respectively. WJ-MSCs fulfilled the criteria of the International Society for Cell and Gene Therapy, indicating successful differentiation towards "osteogenic", "adipogenic" and "chondrogenic" lineages, positive expression (> 95%) for CD73, CD90 and CD105, and negative expression (< 3%) for CD34, CD45 and HLA-DR. WJ-MSCs were successfully differentiated into VSMCs using UCB-PL and ascorbic acid. Differentiated VSMCs expressed *ACTA2, MYOCD, MYH11* and *TGLN*. In addition, early and late VSMCs markers such as ACTA2 and MYH11 were evaluated according to indirect immunofluorescence analyses. HUAs were effectively decellularized and characterized by the preservation of ECM proteins, while no cell and nuclei materials were evident. Statistically significant differences were observed between non-decellularized and decellularized hUAs regarding the hydroxyproline ($P < 0.001$), sGAG ($P < 0.001$) and DNA ($P < 0.001$) content. Decellularized hUAs were successfully repopulated by the produced VSMCs, as it was indicated by histological analysis (H and E, MYH11/DAPI). Repopulated vessels were characterized by elevated levels of hydroxyproline (86 ± 8 μg hydroxyproline/mg of dry tissue weight), sGAG (3 ± 1 μg sGAG / mg of dry tissue weight), and DNA (554 ± 49 ng DNA/mg of dry tissue weight) content after 3 wk of cultivation. In addition, the key proliferation markers Ki67 and proliferating cell nuclear antigen were positively expressed by VSMCs in repopulated vessels, according to immunohistochemistry results.

Research conclusions

VSMCs can be successfully produced from WJ-MSCs using UCB-PL in combination with ascorbic acid. Unlike current approaches, including the exogenous supplementation of growth factors or the use of iPSC technology, no such approaches were applied to this study. UCB-PL contains significant amounts of key growth factors required for VSMC differentiation. In addition, ascorbic acid supplementation to the differentiation medium appears to enhance the underlying mechanism. Besides, the successful production of VSMCs and the development of functional small diameter vascular grafts were assessed. HUAs were efficiently decellularized, and could serve as potential scaffolds for blood vessel engineering. To obtain functional small diameter vascular grafts, the decellularized hUAs were repopulated with the produced VSMCs. Finally, the repopulated vessels were characterized for their similar properties to the hUAs before the decellularization process. Taking into consideration the above data, hUCs could be a rich source both for cellular populations and vessel conduits. Additionally, this study brings into light a safer differentiation process that can possibly be used for the production of patient-specific VSMCs. It is known that the circulatory system of CAD patients is primarily affected. The isolation of VSMCs from patient vessel biopsies, which can be used for vascular graft engineering, is not efficient. On the contrary, MSCs (in adults) that are presented both in bone marrow and adipose tissue, can be isolated and differentiated into VSMCs with the current protocol, and can thus potentially be used in blood vessel engineering. In this way, and unlike the complicated and expensive approaches of the past, the production of fully functional blood vessels is one step closer to its clinical application.

Research perspectives

The next step of this study will be focused on the use of the repopulated (with VSMCs) vascular grafts in an animal model, in order to better evaluate their functionality. Small blood vessel engineering is one of the milestones of personalized regenerative medicine. To this direction, the production of patient-specific small diameter vascular grafts under good manufacturing practice conditions, that can be readily accessible, will be of great importance.

REFERENCES

1 **Pashneh-Tala S**, MacNeil S, Claeyssens F. The Tissue-Engineered Vascular Graft-Past, Present, and Future. *Tissue Eng Part B Rev* 2016; **22**: 68-100 [PMID: 26447530 DOI: 10.1089/ten.teb.2015.0100]

2 **Ong CS**, Zhou X, Huang CY, Fukunishi T, Zhang H, Hibino N. Tissue engineered vascular grafts: current state of the field. *Expert Rev Med Devices* 2017; **14**: 383-392 [PMID: 28447487 DOI: 10.1080/17434440.2017.1324293]

3 **Gui L**, Muto A, Chan SA, Breuer CK, Niklason LE. Development of decellularized human umbilical arteries as small-diameter vascular grafts. *Tissue Eng Part A* 2009; **15**: 2665-2676 [PMID: 19207043]

4 **Mallis P**, Gontika I, Poulogiannopoulos T, Zoidakis J, Vlahou A, Michalopoulos E, Chatzistamatiou T, Papassavas A, Stavropoulos-Giokas C. Evaluation of decellularization in umbilical cord artery. *Transplant Proc* 2014; **46**: 3232-3239 [PMID: 25420867 DOI: 10.1016/j.transproceed.2014.10.027]

5 **Carrabba M**, Madeddu P. Current Strategies for the Manufacture of Small Size Tissue Engineering Vascular Grafts. *Front Bioeng Biotechnol* 2018; **6**: 41 [PMID: 29721495 DOI: 10.3389/fbioe.2018.00041]

6 **Peck M**, Gebhart D, Dusserre N, McAllister TN, L'Heureux N. The evolution of vascular tissue engineering and current state of the art. *Cells Tissues Organs* 2012; **195**: 144-158 [PMID: 21996786 DOI: 10.1159/000331406]

7 **Seifu DG**, Purnama A, Mequanint K, Mantovani D. Small-diameter vascular tissue engineering. *Nat Rev Cardiol* 2013; **10**: 410-421 [PMID: 23689702 DOI: 10.1038/nrcardio.2013.77]
8 **Sánchez PF**, Brey EM, Briceño JC. Endothelialization mechanisms in vascular grafts. *J Tissue Eng Regen Med* 2018; **12**: 2164-2178 [PMID: 30079631 DOI: 10.1002/term.2747]
9 **D Levit R**. Engineering Vessels as Good as New? *JACC Basic Transl Sci* 2018; **3**: 119-121 [PMID: 30062199 DOI: 10.1016/j.jacbts.2017.11.008]
10 **Lin CH**, Hsia K, Ma H, Lee H, Lu JH. In Vivo Performance of Decellularized Vascular Grafts: A Review Article. *Int J Mol Sci* 2018; **19** [PMID: 30029536 DOI: 10.3390/ijms19072101]
11 **Cunnane EM**, Weinbaum JS, O'Brien FJ, Vorp DA. Future Perspectives on the Role of Stem Cells and Extracellular Vesicles in Vascular Tissue Regeneration. *Front Cardiovasc Med* 2018; **5**: 86 [PMID: 30018970 DOI: 10.3389/fcvm.2018.00086]
12 **Chan XY**, Elliott MB, Macklin B, Gerecht S. Human Pluripotent Stem Cells to Engineer Blood Vessels. *Adv Biochem Eng Biotechnol* 2018; **163**: 147-168 [PMID: 29090328 DOI: 10.1007/10_2017_28]
13 **Boroujeni ME**, Gardaneh M. Umbilical cord: an unlimited source of cells differentiable towards dopaminergic neurons. *Neural Regen Res* 2017; **12**: 1186-1192 [PMID: 28852404 DOI: 10.4103/1673-5374.211201]
14 **Alfirevic Z**, Stampalija T, Dowswell T. Fetal and umbilical Doppler ultrasound in high-risk pregnancies. *Cochrane Database Syst Rev* 2017; **6**: CD007529 [PMID: 28613398 DOI: 10.1002/14651858.CD007529.pub4]
15 **DeFreitas MJ**, Mathur D, Seeherunvong W, Cano T, Katsoufis CP, Duara S, Yasin S, Zilleruelo G, Rodriguez MM, Abitbol CL. Umbilical artery histomorphometry: a link between the intrauterine environment and kidney development. *J Dev Orig Health Dis* 2017; **8**: 349-356 [PMID: 28260559 DOI: 10.1017/S2040174417000113]
16 **Chakhunashvili K**, Kiladze M, G Chakhunashvili D, Karalashvili L, Kakabadze Z. A three-dimensional scaffold from decellularized human umbilical artery for bile duct reconstruction. *Ann Ital Chir* 2019; **90**: 165-173 [PMID: 30530984]
17 **Mallis P**, Michalopoulos E, Dinou A, Vlachou MS, Panagouli E, Papapanagiotou A, Kassi E, Giokas CS. Development of HLA-matched vascular grafts utilizing decellularized human umbilical artery. *Hum Immunol* 2018; **79**: 855-860 [PMID: 30213613 DOI: 10.1016/j.humimm.2018.09.001]
18 **Rodríguez-Rodríguez VE**, Martínez-González B, Quiroga-Garza A, Reyes-Hernández CG, de la Fuente-Villarreal D, de la Garza-Castro O, Guzmán-López S, Elizondo-Omaña RE. Human Umbilical Vessels: Choosing the Optimal Decellularization Method. *ASAIO J* 2018; **64**: 575-580 [PMID: 29095734 DOI: 10.1097/MAT.0000000000000715]
19 **Tuan-Mu HY**, Yu CH, Hu JJ. On the decellularization of fresh or frozen human umbilical arteries: implications for small-diameter tissue engineered vascular grafts. *Ann Biomed Eng* 2014; **42**: 1305-1318 [PMID: 24682764 DOI: 10.1007/s10439-014-1000-1]
20 **Takakura N**. Discovery of a Vascular Endothelial Stem Cell (VESC) Population Required for Vascular Regeneration and Tissue Maintenance. *Circ J* 2018; **83**: 12-17 [PMID: 30487375 DOI: 10.1253/circj.CJ-18-1180]
21 **Yue H**, Febbraio M, Klenotic PA, Kennedy DJ, Wu Y, Chen S, Gohara AF, Li O, Belcher A, Kuang B, McIntyre TM, Silverstein RL, Li W. CD36 Enhances Vascular Smooth Muscle Cell Proliferation and Development of Neointimal Hyperplasia. *Arterioscler Thromb Vasc Biol* 2019; **39**: 263-275 [PMID: 30567481 DOI: 10.1161/ATVBAHA.118.312186]
22 **Li M**, Qian M, Kyler K, Xu J. Endothelial-Vascular Smooth Muscle Cells Interactions in Atherosclerosis. *Front Cardiovasc Med* 2018; **5**: 151 [PMID: 30406116 DOI: 10.3389/fcvm.2018.00151]
23 **Zhang X**, Bendeck MP, Simmons CA, Santerre JP. Deriving vascular smooth muscle cells from mesenchymal stromal cells: Evolving differentiation strategies and current understanding of their mechanisms. *Biomaterials* 2017; **145**: 9-22 [PMID: 28843066 DOI: 10.1016/j.biomaterials.2017.08.028]
24 **Zhang L**, Xu Q. Stem/Progenitor cells in vascular regeneration. *Arterioscler Thromb Vasc Biol* 2014; **34**: 1114-1119 [PMID: 24828515 DOI: 10.1161/ATVBAHA.114.303809]
25 **Sata M**. Circulating vascular progenitor cells contribute to vascular repair, remodeling, and lesion formation. *Trends Cardiovasc Med* 2003; **13**: 249-253 [PMID: 12922022]
26 **Kumar A**, D'Souza SS, Moskvin OV, Toh H, Wang B, Zhang J, Swanson S, Guo LW, Thomson JA, Slukvin II. Specification and Diversification of Pericytes and Smooth Muscle Cells from Mesenchymoangioblasts. *Cell Rep* 2017; **19**: 1902-1916 [PMID: 28564607 DOI: 10.1016/j.celrep.2017.05.019]
27 **Biel NM**, Santostefano KE, DiVita BB, El Rouby N, Carrasquilla SD, Simmons C, Nakanishi M, Cooper-DeHoff RM, Johnson JA, Terada N. Vascular Smooth Muscle Cells From Hypertensive Patient-Derived Induced Pluripotent Stem Cells to Advance Hypertension Pharmacogenomics. *Stem Cells Transl Med* 2015; **4**: 1380-1390 [PMID: 26494780 DOI: 10.5966/sctm.2015-0126]
28 **Iso Y**, Usui S, Toyoda M, Spees JL, Umezawa A, Suzuki H. Bone marrow-derived mesenchymal stem cells inhibit vascular smooth muscle cell proliferation and neointimal hyperplasia after arterial injury in rats. *Biochem Biophys Rep* 2018; **16**: 79-87 [PMID: 30377672 DOI: 10.1016/j.bbrep.2018.10.001]
29 **Christou I**, Mallis P, Michalopoulos E, Chatzistamatiou T, Mermelekas G, Zoidakis J, Vlahou A, Stavropoulos-Giokas C. Evaluation of Peripheral Blood and Cord Blood Platelet Lysates in Isolation and Expansion of Multipotent Mesenchymal Stromal Cells. *Bioengineering (Basel)* 2018; **5** [PMID: 29495420 DOI: 10.3390/bioengineering5010019]
30 **Dominici M**, Le Blanc K, Mueller I, Slaper-Cortenbach I, Marini F, Krause D, Deans R, Keating A, Prockop Dj, Horwitz E. Minimal criteria for defining multipotent mesenchymal stromal cells. The International Society for Cellular Therapy position statement. *Cytotherapy* 2006; **8**: 315-317 [PMID: 16923606 DOI: 10.1080/14653240600855905]
31 **Grogan SP**, Barbero A, Winkelmann V, Rieser F, Fitzsimmons JS, O'Driscoll S, Martin I, Mainil-Varlet P. Visual histological grading system for the evaluation of in vitro-generated neocartilage. *Tissue Eng* 2006; **12**: 2141-2149 [PMID: 16968155 DOI: 10.1089/ten.2006.12.2141]
32 **Ma J**, Wu J, Han L, Jiang X, Yan L, Hao J, Wang H. Comparative analysis of mesenchymal stem cells derived from amniotic membrane, umbilical cord, and chorionic plate under serum-free condition. *Stem Cell Res Ther* 2019; **10**: 19 [PMID: 30635045 DOI: 10.1186/s13287-018-1104-x]
33 **Xu Z**, Ji G, Shen J, Wang X, Zhou J, Li L. SOX9 and myocardin counteract each other in regulating vascular smooth muscle cell differentiation. *Biochem Biophys Res Commun* 2012; **422**: 285-290 [PMID: 22580282 DOI: 10.1016/j.bbrc.2012.04.149]
34 **Talele NP**, Fradette J, Davies JE, Kapus A, Hinz B. Expression of α-Smooth Muscle Actin Determines the

Fate of Mesenchymal Stromal Cells. *Stem Cell Reports* 2015; **4**: 1016-1030 [PMID: 26028530 DOI: 10.1016/j.stemcr.2015.05.004]

35 **de la Garza-Rodea AS**, van der Velde-van Dijke I, Boersma H, Gonçalves MA, van Bekkum DW, de Vries AA, Knaän-Shanzer S. Myogenic properties of human mesenchymal stem cells derived from three different sources. *Cell Transplant* 2012; **21**: 153-173 [PMID: 21669036 DOI: 10.3727/096368911X580554]

36 **You JS**, Kelly TK, De Carvalho DD, Taberlay PC, Liang G, Jones PA. OCT4 establishes and maintains nucleosome-depleted regions that provide additional layers of epigenetic regulation of its target genes. *Proc Natl Acad Sci USA* 2011; **108**: 14497-14502 [PMID: 21844352 DOI: 10.1073/pnas.1111309108]

37 **Cheung C**, Bernardo AS, Trotter MW, Pedersen RA, Sinha S. Generation of human vascular smooth muscle subtypes provides insight into embryological origin-dependent disease susceptibility. *Nat Biotechnol* 2012; **30**: 165-173 [PMID: 22252507 DOI: 10.1038/nbt.2107]

38 **Patsch C**, Challet-Meylan L, Thoma EC, Urich E, Heckel T, O'Sullivan JF, Grainger SJ, Kapp FG, Sun L, Christensen K, Xia Y, Florido MH, He W, Pan W, Prummer M, Warren CR, Jakob-Roetne R, Certa U, Jagasia R, Freskgård PO, Adatto I, Kling D, Huang P, Zon LI, Chaikof EL, Gerszten RE, Graf M, Iacone R, Cowan CA. Generation of vascular endothelial and smooth muscle cells from human pluripotent stem cells. *Nat Cell Biol* 2015; **17**: 994-1003 [PMID: 26214132 DOI: 10.1038/ncb3205]

39 **Karamariti E**, Margariti A, Winkler B, Wang X, Hong X, Baban D, Ragoussis J, Huang Y, Han JD, Wong MM, Sag CM, Shah AM, Hu Y, Xu Q. Smooth muscle cells differentiated from reprogrammed embryonic lung fibroblasts through DKK3 signaling are potent for tissue engineering of vascular grafts. *Circ Res* 2013; **112**: 1433-1443 [PMID: 23529184 DOI: 10.1161/CIRCRESAHA.111.300415]

40 **Wanjare M**, Agarwal N, Gerecht S. Biomechanical strain induces elastin and collagen production in human pluripotent stem cell-derived vascular smooth muscle cells. *Am J Physiol Cell Physiol* 2015; **309**: C271-C281 [PMID: 26108668 DOI: 10.1152/ajpcell.00366.2014]

41 **Iyer D**, Gambardella L, Bernard WG, Serrano F, Mascetti VL, Pedersen RA, Talasila A, Sinha S. Robust derivation of epicardium and its differentiated smooth muscle cell progeny from human pluripotent stem cells. *Development* 2015; **142**: 1528-1541 [PMID: 25813541 DOI: 10.1242/dev.119271]

42 **Zhang J**, Lian Q, Zhu G, Zhou F, Sui L, Tan C, Mutalif RA, Navasankari R, Zhang Y, Tse HF, Stewart CL, Colman A. A human iPSC model of Hutchinson Gilford Progeria reveals vascular smooth muscle and mesenchymal stem cell defects. *Cell Stem Cell* 2011; **8**: 31-45 [PMID: 21185252 DOI: 10.1016/j.stem.2010.12.002]

43 **Bajpai VK**, Mistriotis P, Loh YH, Daley GQ, Andreadis ST. Functional vascular smooth muscle cells derived from human induced pluripotent stem cells via mesenchymal stem cell intermediates. *Cardiovasc Res* 2012; **96**: 391-400 [PMID: 22941255 DOI: 10.1093/cvr/cvs253]

44 **Crapo PM**, Gilbert TW, Badylak SF. An overview of tissue and whole organ decellularization processes. *Biomaterials* 2011; **32**: 3233-3243 [PMID: 21296410 DOI: 10.1016/j.biomaterials.2011.01.057]

45 **Theodoridis K**, Müller J, Ramm R, Findeisen K, Andrée B, Korossis S, Haverich A, Hilfiker A. Effects of combined cryopreservation and decellularization on the biomechanical, structural and biochemical properties of porcine pulmonary heart valves. *Acta Biomater* 2016; **43**: 71-77 [PMID: 27422199 DOI: 10.1016/j.actbio.2016.07.013]

46 **Mallis P**, Michalopoulos E, Pantsios P, Kozaniti F, Deligianni D, Papapanagiotou A, Stavropoulos Giokas C. Recellularization potential of small diameter vascular grafts derived from human umbilical artery. *Biomed Mater Eng* 2019; **30**: 61-71 [PMID: 30530958 DOI: 10.3233/BME-181033]

47 **Merfeld-Clauss S**, Lupov IP, Lu H, Feng D, Compton-Craig P, March KL, Traktuev DO. Adipose stromal cells differentiate along a smooth muscle lineage pathway upon endothelial cell contact via induction of activin A. *Circ Res* 2014; **115**: 800-809 [PMID: 25114097 DOI: 10.1161/CIRCRESAHA.115.304026]

Published By Baishideng Publishing Group Inc
7041 Koll Center Parkway, Suite 160, Pleasanton, CA 94566, USA
Telephone: +1-925-3991568
E-mail: bpgoffice@wjgnet.com
Help Desk: https://www.f6publishing.com/helpdesk
https://www.wjgnet.com